Posttreatment Intervention With *Lycium Barbarum* Polysaccharides is Neuroprotective in a Rat Model of Chronic Ocular Hypertension

Yamunadevi Lakshmanan,[1] Francisca Siu Yin Wong,[1] Bing Zuo,[2] Kwok-Fai So,[3,4] Bang Viet Bui,[5] and Henry Ho-Lung Chan[1,2]

[1]Laboratory of Experimental Optometry (Neuroscience), School of Optometry, The Hong Kong Polytechnic University, Hong Kong SAR, China
[2]Centre for Myopia Research, School of Optometry, The Hong Kong Polytechnic University, Hong Kong SAR, China
[3]Department of Ophthalmology, LKS Faculty of Medicine, The University of Hong Kong, Hong Kong SAR, China
[4]Guangdong-Hongkong-Macau (GHM) Institute of CNS Regeneration, Jinan University, Guangzhou, China
[5]Department of Optometry and Vision Sciences, University of Melbourne, Melbourne, Australia

Correspondence: Henry Ho-Lung Chan, School of Optometry, The Hong Kong Polytechnic University, 11, Yuk Choi Road, Hung Hom, Kowloon, Hong Kong SAR; henryhl.chan@polyu.edu.hk.

Submitted: July 2, 2019
Accepted: October 1, 2019

Citation: Lakshmanan Y, Wong FSY, Zuo B, So K-F, Bui BV, Chan HH-L. Posttreatment intervention with *Lycium barbarum* polysaccharides is neuroprotective in a rat model of chronic ocular hypertension. *Invest Ophthalmol Vis Sci*. 2019;60:4606–4618. https://doi.org/10.1167/iovs.19-27886

Purpose. To investigate the neuroprotective effects of *Lycium barbarum* polysaccharides (LBP) against chronic ocular hypertension (OHT) in rats and to consider if effects differed when treatment was applied before (pretreatment) or during (posttreatment) chronic IOP elevation.

Methods. Sprague-Dawley rats (10-weeks old) underwent suture implantation around the limbus for 15 weeks (OHT) or 1 day (sham). Four experimental groups were studied, three OHT groups ($n = 8$ each) treated either with vehicle (PBS), LBP pretreatment or posttreatment, and a sham control ($n = 5$) received no treatment. LBP (1 mg/kg) pre- and posttreatment were commenced at 1 week before and 4 weeks after OHT induction, respectively. Treatments continued up through week 15. IOP was monitored twice weekly for 15 weeks. Optical coherence tomography and ERG were measured at baseline, week 4, 8, 12, and 15. Eyes were collected for ganglion cell layer (GCL) histologic analysis at week 15.

Results. Suture implantation successfully induced approximately 50% IOP elevation and the cumulative IOP was similar between the three OHT groups. When compared with vehicle control (week 4: $-23 \pm 5\%$, $P = 0.03$), LBP pretreatment delayed the onset of retinal nerve fiber layer (RNFL) thinning (week 4, 8: $-2 \pm 7\%$, $-11 \pm 3\%$, $P > 0.05$) and arrested further reduction up through week 15 ($-10 \pm 4\%$, $P > 0.05$). LBP posttreatment intervention showed no significant change in rate of loss (week 4, 15: $-25 \pm 4.1\%$, $-28 \pm 3\%$). However, both LBP treatments preserved the retinal ganglion cells (RGC) and retinal functions up to week 15, which were significantly reduced in vehicle control.

Conclusions. LBP posttreatment arrested the subsequent neuronal degeneration after treatment commencement and preserved RGC density and retinal functions in a chronic OHT model, which was comparable with pretreatment outcomes.

Keywords: glaucoma, neuroprotection, lycium polysaccharides, posttreatment, chronic rat model

Glaucoma is a chronic age-related neurodegenerative disease, characterized by damage to the retinal ganglion cell layer (GCL), leading to progressive vision loss and compromised quality of life. The prevalence of glaucoma is estimated to increase steadily from 60.5 million in 2010 to 111.8 million by 2040,[1] which has significant socioeconomic implications.[2–4] Currently, IOP lowering remains the mainstay treatment for preserving vision, irrespective of the type and severity of glaucoma presentation.[5–7] However, a proportion of patients continue to experience gradual deterioration in vision despite well-managed IOP.[5–7] Hence, adjuncts to IOP lowering, such neuroprotective strategies are needed to preserve healthy neurons and rescue damaged neurons.[8,9]

While it is not fully understood why ageing predisposes to glaucoma, increased oxidative stress is thought to play a significant role.[10–14] It is well-documented that as cell ages, there is an increased level of free radicals, which can compromise mitochondrial energy production and normal neuronal functioning.[15,16] Thus, complementary and alternate medicines that seek to ameliorate energy deprivation and reduce oxidative stress have been sought as therapeutic targets for glaucoma treatment.[17–19] In recent years, traditional Chinese medicines have received considerable interest for their potential neuroprotective effects in neurodegenerative disease, including glaucoma.[20] Potentially useful are the polysaccharides extracted from the fruits of *Lycium barbarum* (wolfberry), which has been reported to be an effective antiaging agent[21,22] with cytoprotective properties[23] and the capacity to modify oxidative stress,[24–26] immune responses,[27,28] and neuronal responses.[29–31] *L. barbarum* polysaccha-

ride (LBP) has shown to protect retinal ganglion cells (RGC) in both IOP-dependent[32–35] and -independent models[36–41] of optic neuropathy. Chan et al.[32] first demonstrated a dose-dependent RGC preservation with LBP pretreatment in an in vivo ocular hypertension (OHT) rat model induced by laser photocoagulation of the trabecular meshwork. A number of studies have since confirm that LBP pretreatment was protective for RGCs in a range of injury models including chronic OHT,[32–35] acute ocular hypertension (AOH),[36,37] partial optic nerve transection,[38–40] and ischemia reperfusion injury.[41] While, the benefits of LBP pretreatment are clear in experimental glaucoma model, treatment in the clinical setting is often initiated once disease risk or the presence of injury has been confirmed.

To better replicate clinical management and to increase the chance for effective translation,[42,43] we sought to assess the potential benefits of LBP intervention in preserving the retinal structure and function when delivered well after the onset of neuronal degeneration. Using the minimally invasive circumlimbal suture model of OHT in rats, we assessed neuroprotective efficacy of LBP when intervention was initiated before (pretreatment) and well after the onset of IOP elevation (posttreatment). In Sprague-Dawley rats, the circumlimbal suture approach facilitated longitudinal assessment, allowing us to demonstrate robust retinal nerve fiber layer (RNFL) thinning and a corresponding reduction in ganglion cell function.[44] Using in vivo longitudinal assessment of retinal structure (optical coherence tomography [OCT]) and function (ERG), we tested the hypothesis that neuroprotective effects of LBP against chronic IOP elevation can be achieved with pre- and posttreatment intervention.

Materials and Methods

Animals

Animal care and experimental procedures were undertaken in accordance with the ARVO Statement for the Use of Animals in Ophthalmic and Vision Research and were approved by the Animal Ethics subcommittee of The Hong Kong Polytechnic University. Female Sprague-Dawley rats of 10 weeks of age, weighing 180 to 210 g at the start of the experiment were housed at room temperature (22°C) under normal lighting condition (~200 lux) with an alternating light/dark cycle (12-hours light/12-hours dark, on at 8 AM). Food (PicoLab diet 20 [5053]; PMI Nutrition International, Richmond, IN, USA) and water were available to animals ad libitum.

Experimental Design

Forty-two Sprague-Dawley rats underwent baseline OCT and ERG examinations, after which they were randomly assigned to one of four experimental groups. These include three OHT groups, namely (1) OHT-vehicle control, in which animals were posttreated with PBS, (2) OHT-LBP pretreatment (preTx), (3) OHT-LBP posttreatment (postTx), and a (4) sham control, which received no treatment. A dosage of 1 mg/kg LBP was used in both LBP pre- and postTx groups. The pretreatment was initiated 1 week prior to OHT induction and posttreatment was commenced 4 weeks after OHT induction. Both LBP treatments were continued up through week 15. At day 0, all the animals underwent OHT induction and longitudinal structural and functional changes were assessed using OCT and ERG, respectively, at the end of weeks 4, 8, 12, and 15. After in vivo assessment at week 15, animals were euthanized by CO_2 asphyxiation and eyes were collected for histologic examination (see Supplementary Fig. S1 for schematic diagram of experimental study design).

IOP Measurements and OHT Induction

IOP was measured in rats using a rebound tonometer (Tonolab; Icare, Vantaa, Finland) and recordings were obtained between 10:30 AM and 12:30 PM to minimize diurnal variations. All animals were handled and acclimatized for 3 days to awake IOP measurements. Baseline IOP was obtained by averaging IOP measurements collected on two subsequent days. On the day of OHT induction (day 0), animals were anesthetized with an intraperitoneal injection of a 60 mg/kg ketamine and 5 mg/kg xylazine mixture (Alfasan International B.V., Woerden, Holland). Following application of a drop of topical anesthetic (Provain-POS 0.5% wt/vol eye drop; URSAPHARM, Saarbrücken, Germany), a circumlimbal suturing was implanted. Briefly, an 8/0 nylon suture was tied around the globe at approximately 1.5 to 2 mm behind the limbus, and secured using six to seven subconjunctival anchor points. The suture was then tightened until IOP reached approximately 70 mm Hg; this was then secured with a second knot. Suture ends were trimmed to minimize irritation and eyes were treated with a topical antibiotic (Gentamicin; Gibco, Thermo-Fisher Scientific, Waltham, MA, USA). The suture was applied in both eyes of the animals assigned to OHT groups and in one randomly selected eye in the sham control group.

On the day after OHT induction (postoperative day 1), the suture was left intact in one randomly selected eye and removed from the other eye. For sham control animals, the suture was removed and the other eye was maintained as a naïve fellow control eye. IOP was monitored on alternate days in the first week and then twice weekly up to week 15. Sutured eyes that maintained an IOP elevation of 25% above the fellow control eyes (suture removed) in the first 4 weeks were considered to be successful OHT induction and were followed up through 15 weeks. Approximately, 30% ($n = 12$) of animals were excluded from the analysis due to inadequately sustained IOP elevation (OHT vehicle control: 3; OHT-LBP PreTx: 2; OHT-LBP PostTx: 3), development of corneal opacities (sham control: 1; OHT vehicle control: 1) or attrition (sham control: 1; OHT-LBP PostTx: 1) during follow-up examinations.

Drug Administration

The method of extracting polysaccharides from Lycium fruit has been detailed elsewhere.[45] Fresh LBP solution was prepared by dissolving dried LBP powder in PBS. Animals were either pre- or posttreated with 1 mg/kg LBP or PBS once daily using a nasogastric feeding tube between 10:30 AM and 11:30 AM. Animals in pre- (weeks −1 to 15) and posttreatment (weeks 5–15) received feeding for a total of 16 and 11 weeks, respectively.

Optical Coherence Tomography

The peripapillary retinal thickness was imaged using a spectral-domain optical coherence tomography (SD-OCT; Micron IV; Phoenix Research Lab, Pleasanton, CA, USA) as described earlier.[46] Briefly, animals were anesthetized with ketamine-xylazine and pupils were dilated (Mydriacyl 1%; Alcon-Couvreue, Puurs, Belgium). A peripapillary B-scan of 0.51-mm radius, consisting of 1024 A-scan with axial and transverse resolutions of 1.8 and 3.0 μm, respectively, was acquired. Images were then analyzed using a semiautomated segmentation algorithm (Insight software; Phoenix Research Lab) to measure the thicknesses of total retina (TRT), retinal nerve fiber layer (RNFLT), inner retinal layer (IRLT), and outer retinal

layers (ORLT). The TRT was measured from the RPE layer to the inner limiting membrane, the IRLT was the total thickness of the inner plexiform and inner nuclear layer (INL), and the ORLT was measured from the RPE layer to the outer plexiform layer.

Electroretinography

Full-field Ganzfeld (Q450; RETI Animal; Roland Consult, Brandenburg an der Havel, Germany) stimuli was used to elicit inner and outer retinal responses from experimental animals as described previously.[46] Briefly, under dim red light, dark adapted animals (>12 hours of dark adaptation) were anaesthetized using ketamine-xylazine and placed on a temperature controlled platform connected to a warm water bath (37°C). Pupils were dilated and a drop of lubricating gel was applied to prevent corneal dehydration. Recordings were taken from both eyes using gold ring electrodes placed on the corneal surface (active electrode) and needles electrodes inserted into the lateral canthi of each eye (reference electrode) and the base of the tail (ground electrode).

The positive scotopic threshold response (pSTR) was measured by averaging 30 (interstimulus interval of 2 seconds) responses using a series of brief (2 μs) dim white light-emitting diode flash intensities ranging from –4.8 to –4.05 log cd.s/m^2 with 0.15-log cd.s/m^2 steps. Scotopic (mixed rod and cone) responses were recorded using a single flash of 1.3 log cd.s/m^2. Signals were recorded with a band pass filter of 0.1 to 1000 Hz. The amplitudes and implicit time of the pSTR, scotopic a- and b-wave responses, which correspond to ganglion, photoreceptor, and bipolar cell function, respectively, were analyzed.

Histologic Examination

At the end of week 15, animals were euthanized by the inhalation of CO_2 and eye cups were collected for histology analysis as reported earlier.[46] Briefly, the eye cups were fixed overnight using 4% paraformaldehyde in PBS at room temperature, after which tissues were dehydrated using graded ethanol before paraffin embedded. Retinal section of 5 μm parallel to the optic nerve were collected, stained with hematoxylin and eosin (H&E), and imaged using a light microscope at ×200 magnifications (Nikon, Tokyo, Japan). The peripheral (250 um away from the ora serrata) and the central (250 um away from the scleral canal opening) retinal regions of 500 × 500 μm along with optic nerve head (ONH) were selected for morphologic analysis. The GCL density (cells/mm) of both central and peripheral retinal regions was calculated by dividing the manually counted cell number in the GCL with the corresponding retinal length measured using ImageJ software (http://imagej.nih.gov/ij/; provided in the public domain by the National Institutes of Health, Bethesda, MD, USA).

Immunohistochemistry

The de-paraffinized retinal sections were blocked with goat serum and incubated with primary mouse anti–β-III-tubulin (1:1000; BioLegend, San Diego, CA, USA) at 4°C overnight. The retinal sections were then incubated with Alexa Fluor 488 goat anti-mouse IgG (1:500; Molecular Probes, Invitrogen, Carlsbad, CA, USA) to visualize the signal and the cell nuclei were counterstained with 4′-6-diamidino-2-phenylindole (DAPI). Stained sections were imaged using a light microscope at ×200 magnifications (Nikon). The RGC density was obtained by manually counting the β-III-tubulin–positive cells from central retinal region of 500 × 500 μm and divided by the corresponding retinal length using ImageJ.

Statistical Analysis

The data collection and analysis were masked. The data were normally distributed and are presented as mean with SD. All analysis was performed using SPSS 23.0 (IBM Corp, Armonk, NY, USA). The significance level was set at $P < 0.05$. A 2-way repeated measure (RM) ANOVA was used to compare the IOP measurements, OCT, and ERG parameters between the experimental and fellow control eyes over time. Cumulative IOP (week 0–15) was calculated for each experimental group and a mixed-model ANOVA was used to compare differences in cumulative IOP within groups (between experimental and fellow eye) and between groups (across different treatment conditions) with Bonferroni correction. To test the long-term protective effects on structural and functional parameters under different treatment conditions, data from treated eyes were first expressed relative to their contralateral control eyes ([experimental eye − fellow control] / fellow control × 100 [%]) and then as a difference (%) from baseline. A mixed-model ANOVA was used to compare the difference in retinal layer thicknesses and ERG parameters (amplitudes and implicit time) among the four groups and also within each group over time. A post hoc comparison between groups or eyes at various time points was undertaken using Bonferroni test.

Results

Comparison of Chronic IOP Elevation by Circumlimbal Suture Model Between Experimental Groups

Baseline IOP was similar in all experimental groups (11 ± 1 mm Hg). After securing the suture, a spike in IOP to 73.0 ± 10 mm Hg was detected in all groups, which dropped by approximately 50% in 10 minutes. Figure 1A shows IOP data for sham control ($n = 5$), which had the suture removed at day 1 and its naïve fellow control eye. IOP returned to normal after suture removal on postoperative day 1 and was similar to the control eye throughout the 15 weeks. Figures 1B to 1D shows IOP measurements from OHT-vehicle control ($n = 8$, Fig. 1B), OHT-LBP pretreatment ($n = 8$, Fig. 1C), and OHT-LBP posttreatment ($n = 8$, Fig. 1D) groups, in which one eye had the suture in place for 15 weeks and the contralateral control eye underwent suture removal at postoperative day 1. IOP in experimental eyes was significantly higher than fellow control eyes in all three OHT groups (2-way RM ANOVA: between eyes: $P = 0.0001$). Figure 1E shows cumulative IOP for control and treated eyes from each experimental group. Cumulative IOP was significantly different between eyes and between experimental groups (mixed ANOVA: between eyes: $P < 0.001$; between groups: $P = 0.01$; interaction: $P < 0.001$). All OHT eyes had approximately 35% higher cumulative IOP compared with their fellow control eyes and sham control eyes ($P < 0.001$). Cumulative IOP was similar among the three OHT groups ($P > 0.05$). Also, there was no difference in cumulative IOP between suture cut sham control eyes and fellow naïve control eyes ($P > 0.05$).

Longitudinal Effect of LBP Treatments on OCT Measured Retinal Layers

Change in thicknesses of the TRT, RNFLT, IRLT, and ORLT over the week 15 for all four experimental groups are expressed as percentage change from baseline (Fig. 2). The raw data of all the retinal thicknesses are presented in Supplementary Figure S2 and the representative SD-OCT B-scans from each experimental group were shown in Supplementary Figure S3. TRT

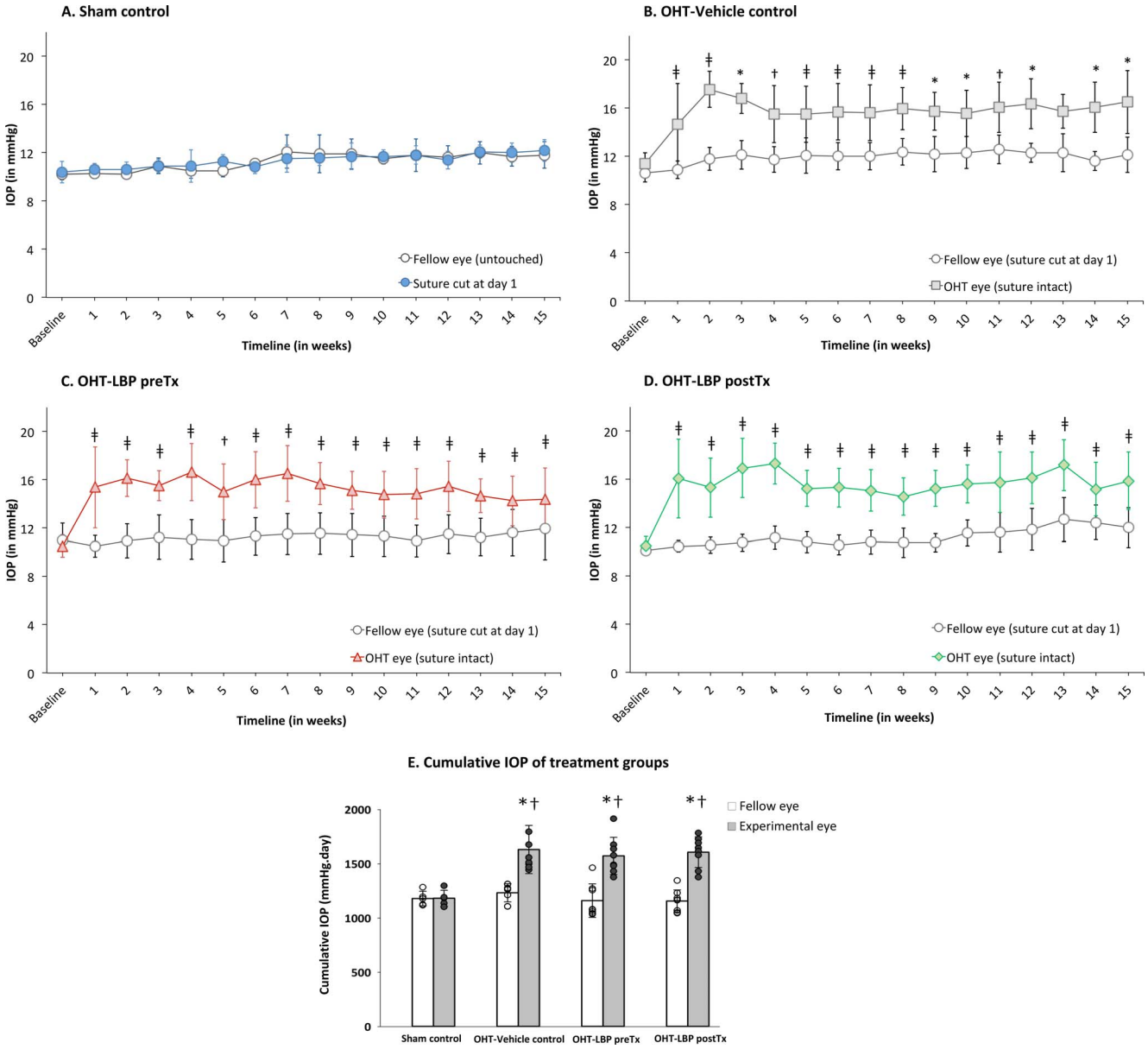

Figure 1. IOP profile of experimental animals over 15 weeks of study. Mean IOP measurements of experimental and fellow eyes were presented for (**A**) sham control, (**B**) OHT-vehicle control, (**C**) OHT-LBP preTx, and (**D**) OHT-LBP postTx animals. *Error bars*, standard deviation. *$P < 0.05$, †$P < 0.01$, ‡$P < 0.001$ versus fellow control (*†‡Bonferroni's post hoc test of 2-way RM ANOVA). (**E**) Cumulative IOP of experimental and fellow eyes among different treatment conditions. *Error bars*, standard deviation. Each *circle* in the bar chart represents individual data points of the animals. *$P < 0.05$ versus fellow eye; †$P < 0.05$ versus sham control (*†mixed-model ANOVA).

(Fig. 2A) was significantly different between treatment groups over time (mixed ANOVA: interaction effect: $P = 0.01$). While the TRT of sham control eyes remained stable over the 15 weeks (week 15: 1.4 ± 1.2%, $P > 0.05$, relative to baseline), the OHT-vehicle control group showed thinning at week 4 (–2.4 ± 2.5%, $P = 0.02$, relative to baseline; $P = 0.01$, compared with sham control). From week 8, there was a gradual thickening of TRT up to week 15 (4.1 ± 4.4%, $P = 0.01$, relative to baseline, weeks 4 and 8). With LBP pretreatment, there was no change in TRT (week 4: –0.3 ± 1.9%, $P > 0.05$; week 15: 2.0 ± 2.8%, $P > 0.05$, relative to baseline). With LBP posttreatment, there was significant TRT thinning at week 4 (–1.6 ± 2.0%, $P = 0.27$, relative to baseline, $P = 0.03$, compared with sham control). However, after commencing LBP posttreatment from week 5, TRT improved and was comparable with baseline up to week 15 (0.8 ± 1.6%, $P > 0.05$, relative to baseline). This was not different to sham controls.

RNFLT (Fig. 2B) differed significantly among experimental groups over time (mixed ANOVA: interaction effect: $P = 0.01$). RNFL thickness of sham controls was not significantly altered (week 15: 6.5 ± 8.4%, $P > 0.05$). Following OHT induction, RNFL thickness in the vehicle-treated group showed significant thinning at week 4 (–23.4 ± 15.3%, $P = 0.03$, relative to baseline; $P = 0.06$, compared with sham control) that was sustained up to week 15 (–17.0 ± 16.6%, $P = 0.04$, relative to baseline). LBP pretreatment prevented RNFLT thinning at week 4 (–2.0 ± 18.9%, $P > 0.05$, relative to baseline). While

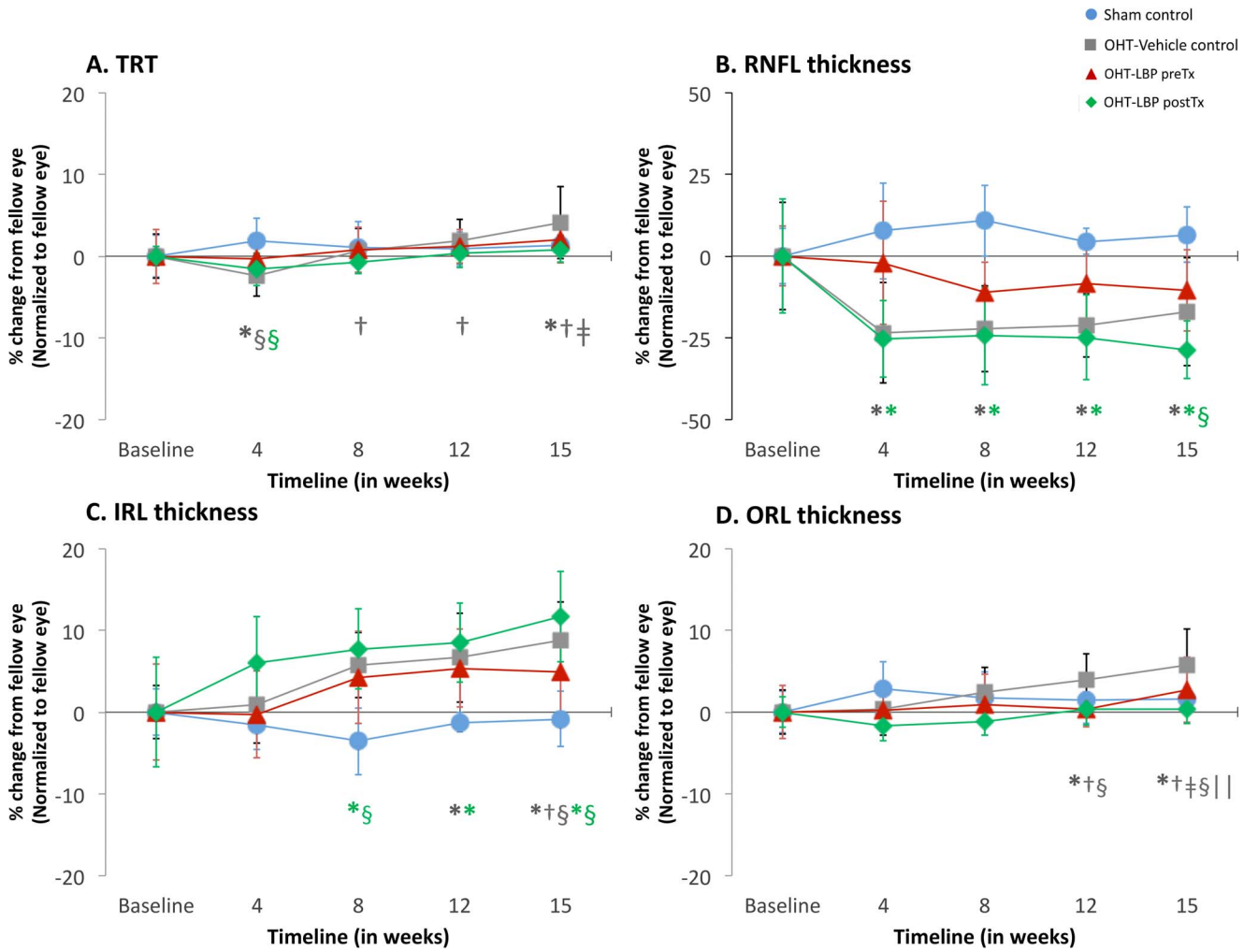

FIGURE 2. Longitudinal effects of OHT and LBP treatment on retinal layer thicknesses measured using OCT. (**A**) TRT, (**B**) RNFL, (**C**) IRL, and (**D**) ORL thicknesses were quantified and compared. Data from experimental eye are expressed as percentage change from fellow control and difference from baseline was compared between different treatment conditions. *Error bars*, standard deviation. *$P < 0.05$ versus baseline; †$P < 0.05$ versus week 4; ‡$P < 0.05$ versus week 8; §P <0 .05 versus sham control; ||$P < 0.05$ versus OHT LBP post-treatment (*†‡§||Bonferroni's post hoc test of mixed-model ANOVA).

not significant, there was a trend for RNFL thinning at week 8 (–11.0 ± 9.1%, $P > 0.05$, relative to baseline) and week 15 (–10.4 ± 12.4%, $P = 0.64$, relative to baseline). In the LBP posttreatment group, there was a significant RNFL thinning at week 4 (–25.3 ± 11.7%, $P = 0.02$, relative to baseline; $P = 0.05$, compared with sham control). After initiating LBP treatment from week 5, there was no further significant change in the rate of RNFL loss (week 15: –28.7 ± 8.9%, $P > 0.05$, relative to week 4). However, RNFL thickness (see Supplementary S2B of OHT-LBP postTx) showed a mild increase in both experimental and fellow controls from weeks 4 (OHT versus fellow eye: 20.3 ± 0.7 µm; 22.8 ± 1.4 µm) to 8 (23.8 ± 1.2 µm, $P = 0.15$; 26.4 ± 1.2 µm; $P = 0.08$, relative to week 4) that was maintained up through week 15 (23.1 ± 0.7 µm, $P = 0.30$; 26.8 ± 1.0 µm, $P = 0.05$, relative to week 4).

The IRLT (Fig 2C) showed a significant interaction effect between treatment and time (mixed ANOVA: interaction effect: $P = 0.02$). While IRLT was stable in sham controls, the OHT-vehicle control showed a gradual increase in thickness from week 8 onward (5.8 ± 4.0%, $P = 0.12$, relative to baseline), which became statistically significant at weeks 12 (6.7 ± 5.5%, $P = 0.04$, relative to baseline) and 15 (8.8 ± 4.7%, $P = 0.001$, relative to baseline; $P = 0.01$, compared with sham control). With LBP pretreatment, while there was a trend for IRLT thickening this was not significant (week 8: 4.3 ± 5.6%, $P = 0.58$; week 15: 4.9 ± 6.4%, $P = 0.15$, relative to baseline). With LBP posttreatment, IRLT was significantly increase from week 8 (7.7 ± 4.9%, $P = 0.01$, relative to baseline; $P = 0.03$, compared with sham control) to week 15 (11.7 ± 5.5%, $P = 0.001$, relative to baseline; $P = 0.001$, compared with sham control).

ORLT (Fig. 2D) was also significantly different between treatment groups (mixed-model ANOVA: interaction effect: $P = 0.001$). While the sham control showed no change in ORLT over the 15 weeks, vehicle-treated OHT eyes showed a significant increase in ORLT at week 12 (4.0 ± 3.2%, $P = 0.01$) and 15 (5.7 ± 4.4%, $P = 0.001$, relative to baseline). No significant changes in ORLT were detected in both LBP treatment groups. At week 15, the thickness of the vehicle control was significantly greater than the sham control ($P = 0.03$) and the OHT-LBP postTx ($P = 0.01$) groups.

Longitudinal Effect of LBP Treatments on ERG Measured Retinal Functions

Figures 3A to 3D show the averaged pSTR responses of animals under different treatment conditions compared with their

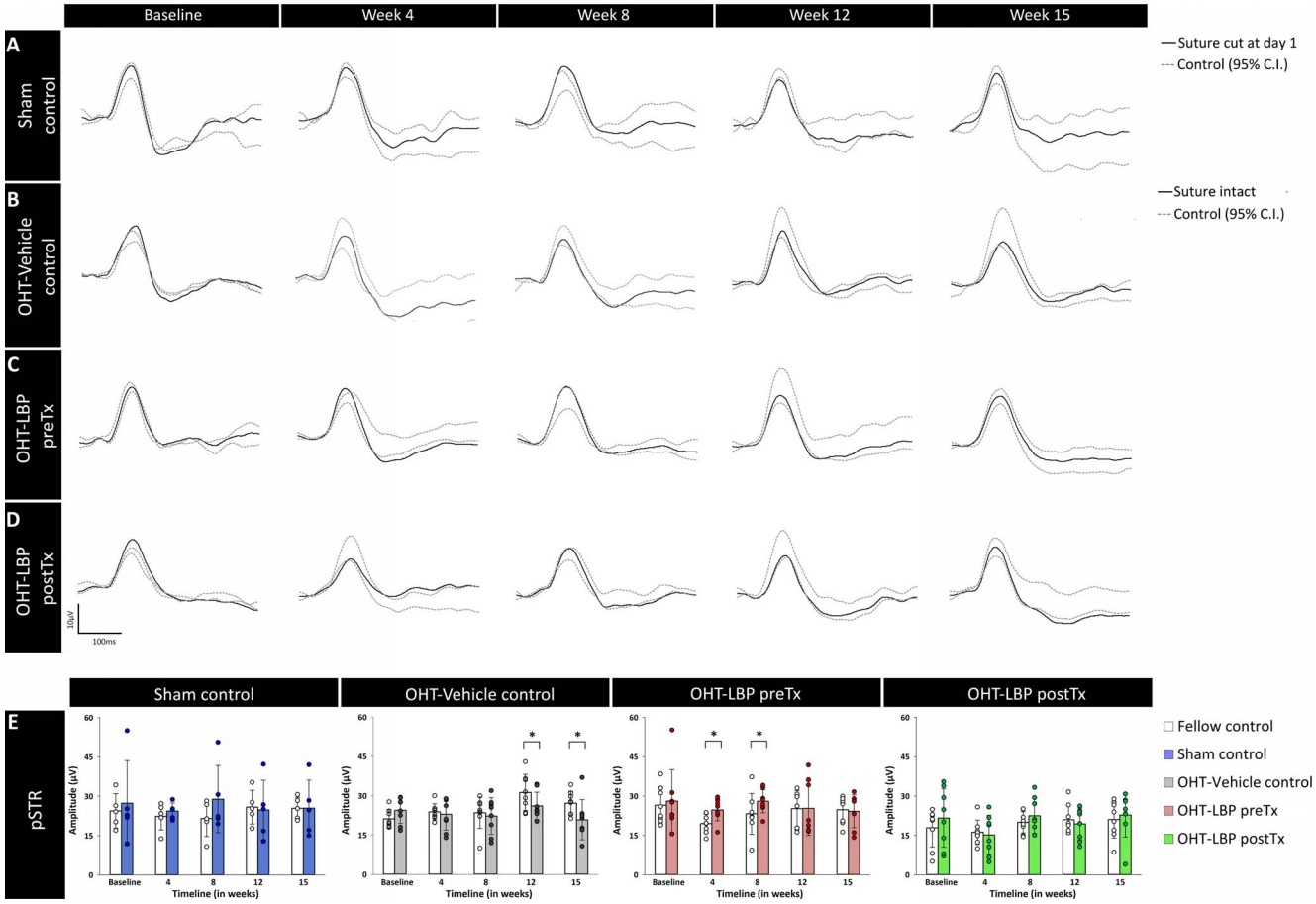

Figure 3. Longitudinal effects of OHT and LBP treatments (1 mg/kg) on the pSTR over 15 weeks of study. (**A**) The pSTR (representing ganglion cell function) of the sham control group remained stable and was comparable with the fellow control. (**B–D**) While the pSTR of OHT-vehicle control (**B**) reduced gradually from week 4 to 15, pretreatment of LBP (**C**) preserved responses up through week 15. Although the pSTR of OHT-postTx showed an initial reduction at week 4, after intervention from week 5, an improvement in the pSTR was observed from week 8 to15. *Black traces* represent the averaged pSTR responses from experimental eyes; *gray dotted traces* indicate the upper and lower limits of the 95%CI of fellow control eyes. (**E**) PSTR amplitudes were compared between experimental and fellow eyes for each treatment group. *Error bars*, standard deviation. Each *circle* in the bar chart represents individual data points of the animals. *$P < 0.05$, †$P < 0.01$, and ‡$P < 0.001$ versus fellow control (*†‡Bonferroni's post hoc test of 2-way RM ANOVA).

respective fellow control eyes (95%CI) from baseline to week 15. The individual data points from each experimental group along with their respective fellow controls from baseline to week 15 are shown in Figure 3E and the amplitudes between eyes are compared for each group (two-way RM ANOVA). While the pSTR responses of sham control were similar between eyes over the 15 weeks, it was reduced in OHT-vehicle–treated animals at weeks 12 ($P = 0.05$) and 15 ($P = 0.04$). With LBP pretreatment, the amplitudes of pSTR in OHT eyes were greater than those in the fellow control eyes at weeks 4 ($P = 0.05$) and 8 ($P = 0.04$), and remained similar to those in the fellow control eyes at weeks 12 and 15. In the LBP posttreatment group, the pSTR showed a trend of mild reduction at week 4. Following LBP treatment from week 5, the amplitudes of OHT eyes improved and were comparable with the fellow eye up through week 15. When comparing the pSTR responses among the treatment groups (mixed ANOVA: time effect: $P = 0.37$; between groups: $P = 0.04$; interaction effect: $P = 0.76$), LBP pretreatment was significantly greater than the OHT-vehicle control ($P = 0.03$).

Figure 4 presents the averaged scotopic ERG traces (Figs. 4A–D) and the individual data points of scotopic b- (Fig. 4E) and a-wave (Fig. 4F) responses of animals from each experimental group, which are compared with their respective fellow control eyes from baseline to week 15 (2-way RM ANOVA). The scotopic responses of sham control were similar between eyes over 15 weeks. While there was no difference in scotopic b-wave response between OHT and fellow eyes in vehicle-treated animals, the a-wave responses were significantly reduced at week 12 ($P = 0.01$) and 15 ($P = 0.04$). With LBP pretreatment, both the scotopic a- and b-waves in OHT eyes were significantly greater than those in the fellow control eyes at weeks 4 ($P = 0.02$) and 8 ($P = 0.01$), which then remained similar between eyes at weeks 12 and 15. In the LBP posttreatment group, scotopic ERG responses were similar between OHT and control eyes, except for week 8, in which they were significantly greater than those of their fellow control eyes ($P = 0.001$). When comparing the scotopic responses between treatment groups, the a-wave (mixed ANOVA: interaction effect: $P = 0.03$) of LBP posttreatment group was significantly reduced at week 4 as compared with the pretreatment ($P = 0.02$). After initiating the LBP treatment from week 5, the responses improved subsequently that showed no difference between treatment groups until week 15. The scotopic b-wave responses were not different between

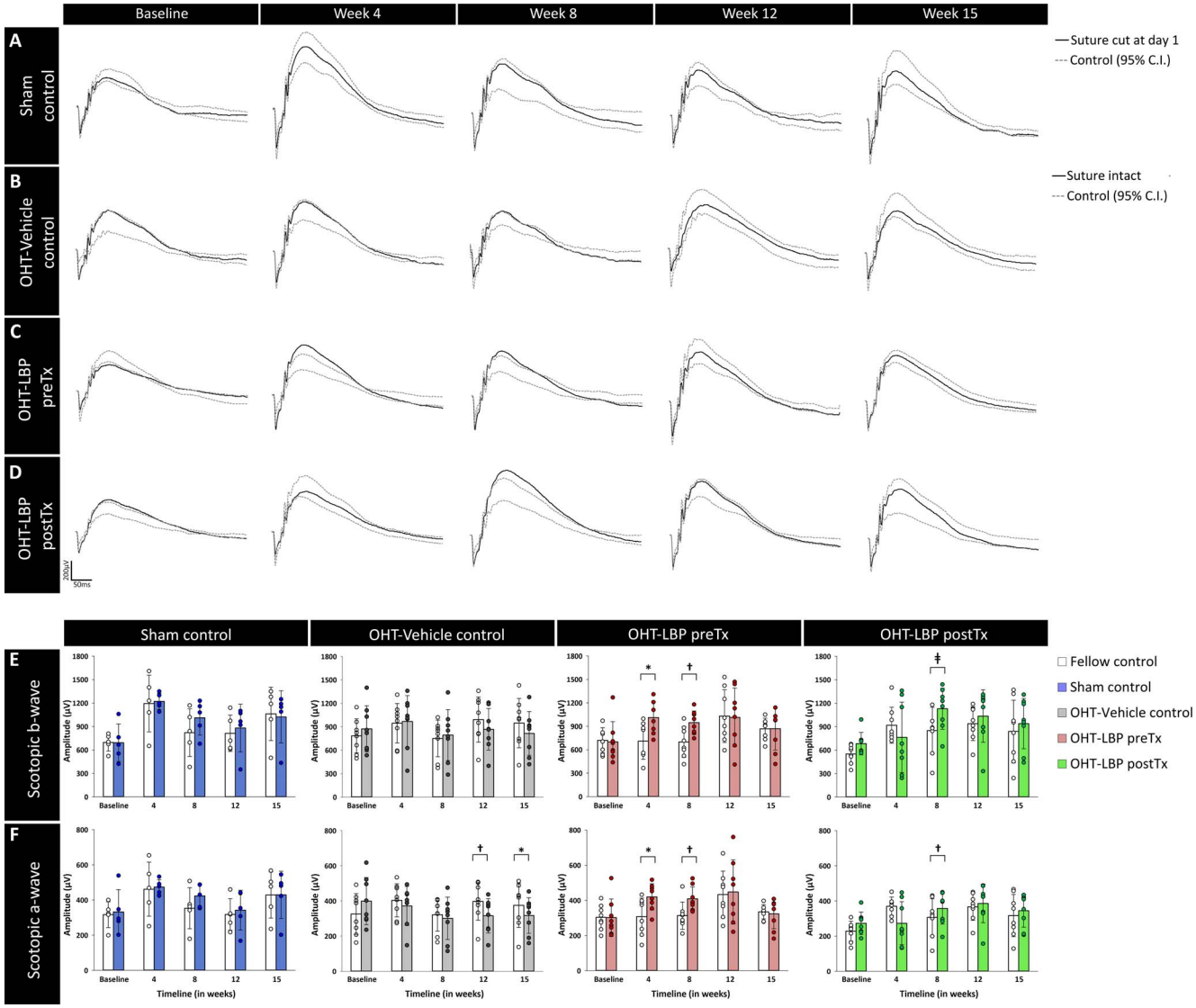

Figure 4. Longitudinal effects of OHT and LBP treatments (1 mg/kg) on scotopic a- and b-wave responses over 15 weeks of study. (**A–D**) The b-wave responses (bipolar cell function) remained stable across all experimental groups. (**B**) Upon OHT induction, the a-wave response (photoreceptor function) of vehicle control showed a reduction from weeks 4 to 15. (**C**, **D**) Both pre- and posttreatments of LBP preserved a-wave responses up through week 15. *Black traces* represent the averaged scotopic responses from the experimental eyes; *gray dotted traces* indicate the upper and lower limits of the 95%CI of the fellow control eyes. The amplitudes of (**E**) scotopic b-wave and (**F**) a-wave responses were compared between experimental and fellow eyes for each treatment group. *Error bars*, standard deviation. Each *circle* in the bar chart represents individual data points of the animals. *$P < 0.05$, †$P < 0.01$, and ‡$P < 0.001$ versus fellow control (*†‡Bonferroni's post hoc test of 2-way RM ANOVA).

the treatment groups (mixed ANOVA: time effect: $P = 0.15$; between groups: $P = 0.29$; interaction effect: $P = 0.19$).

The implicit time of the all the three ERG responses were not significantly different between the experimental groups (mixed ANOVA: interaction effect: $P > 0.05$) and data were shown in Supplementary Figure S4.

Effect of LBP Treatments on Preservation of GCL Density and Axonal Arrangements

Figure 5 shows H&E-stained central and peripheral retinal cross sections for one representative eye from each experimental group. Retinal layers were grossly similar among experimental groups. However, the GCL density (Fig. 5D) of central retina in the experimental eyes differed significantly among treatment groups (mixed ANOVA: between eye: $P = 0.22$; between groups: $P = 0.01$; interaction: $P = 0.22$). Following OHT induction, GCL density in vehicle-treated OHT eyes was significantly reduced compared with fellow control eyes ($P = 0.02$), sham control eyes ($P = 0.03$), and LBP pretreatment OHT eyes ($P = 0.01$). Both LBP-treated groups showed GCL densities similar to their fellow control eyes or the sham control eyes. GCL density in the peripheral retina (Fig. 5C) was not significantly different between the treatment groups (mixed ANOVA: between eyes: $P = 0.08$; between groups: $P = 0.81$; interaction: $P = 0.47$). However, GCL density in OHT-vehicle control eyes was significantly reduced compared with their fellow control eyes ($P = 0.03$).

As GCL density reflects changes in both RGC and amacrine cells,[47] the retinal sections were also stained with β-III-tubulin, an RGC specific marker. Figure 6 shows the representative immunostained retinal sections with β-III-tubulin from each

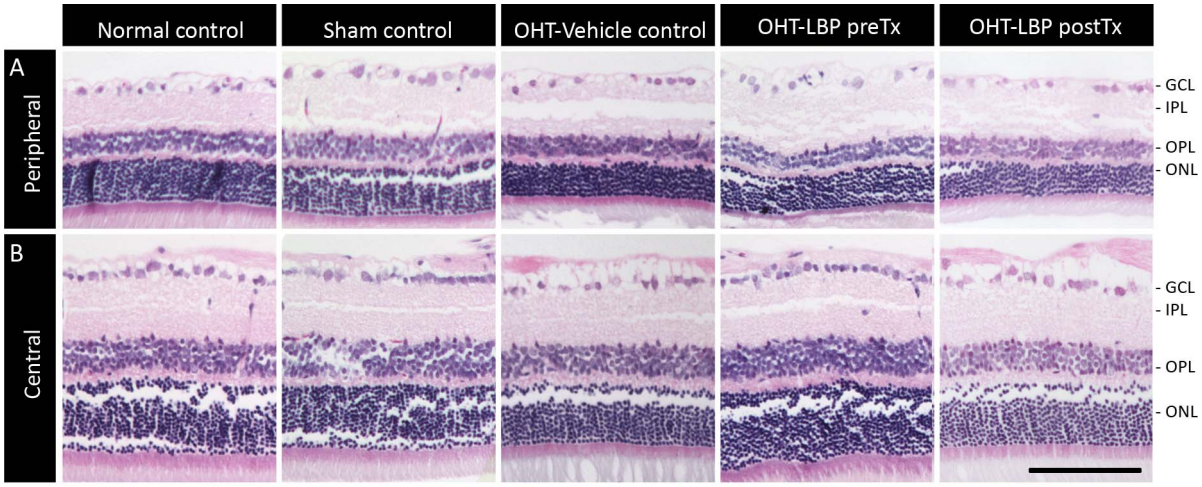

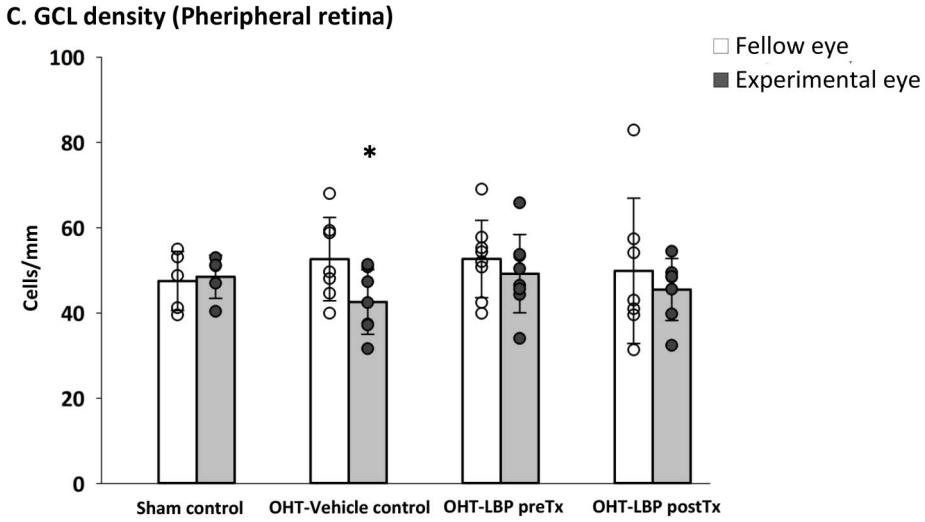

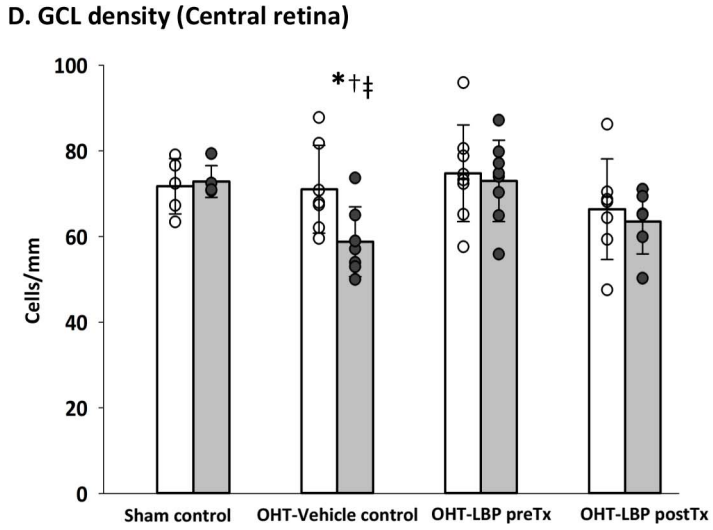

Figure 5. Morphologic rescue effect of LBP pre- and posttreatments at week 15. (**A**, **B**) H&E–stained (**A**) peripheral and (**B**) central retina of one representative rat from each experimental group. (**C**, **D**) Mean GCL densities in the peripheral (**C**) and the central (**D**) retinal sections were quantified for each experimental group and were compared with the fellow eye. *Error bars*, standard deviation. Each *circle* in the bar chart represents individual data points of the animals. $^{*}P < 0.05$ versus fellow eye; $\dagger P < 0.05$ versus sham control; $\ddagger P < 0.05$ versus OHT LBP pretreatment (*†‡Bonferroni post hoc test of mixed-model ANOVA). *Scale bar*: 100 µm. IPL, inner plexiform layer; INL, inner nuclear layer; OPL, outer plexiform layer; ONL, outer nuclear layer.

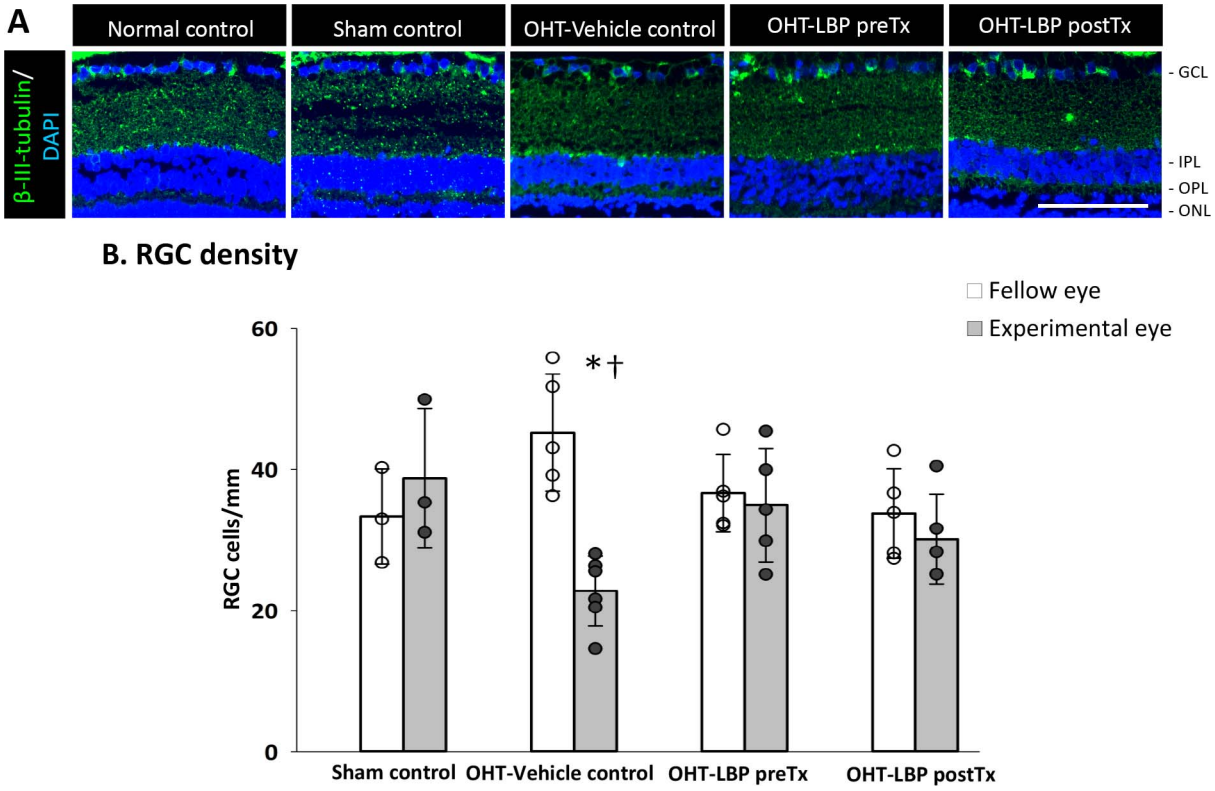

Figure 6. Neuroprotective effects of LBP pre- and posttreatment on RGCs. (**A**) Immunofluorescent staining with anti–β-III-tubulin and DAPI nuclear counterstain of one representative rat retina from each experimental group. (**B**) Mean RGC densities were quantified for each experimental group and were compared with the fellow eye ($n = 3$, 6, 5, and 5 rats for sham control, OHT-vehicle control, pre-, and posttreatment, respectively). *Error bars*, standard deviation. Each *circle* in the bar chart represents individual data points of the animals. *$P < 0.05$ versus fellow eye; †$P < 0.05$ versus sham control (*†Bonferroni post hoc test of mixed-model ANOVA). *Scale bar*: 100 µm.

experimental group. The RGC density (Fig. 6B) in the central retina was significantly reduced in the OHT-vehicle control (mixed ANOVA: between eye: $P = 0.02$; between groups: $P = 0.61$; interaction: $P = 0.002$) as compared with its fellow control ($P = 0.001$) and the sham control ($P = 0.03$). The RGC densities of both LBP-treated groups were similar to their fellow control eyes and the sham control. These results were comparable with the GCL density quantified from H&E-stained sections.

Examination of the optic nerve sections showed that the OHT-vehicle control eyes showed disruption of axon bundle structure and posterior deformation of the ONH surface. In OHT-LBP preTx eyes, axonal bundle arrangement was maintained. In LBP posttreated OHT eyes, there also appeared to be preservation of axon bundle structure (Fig. 7).

Discussion

The present study was the first to directly compare pre- and posttreatment intervention with LBP in a rat model of chronic OHT. We show that both pre- and posttreatment intervention

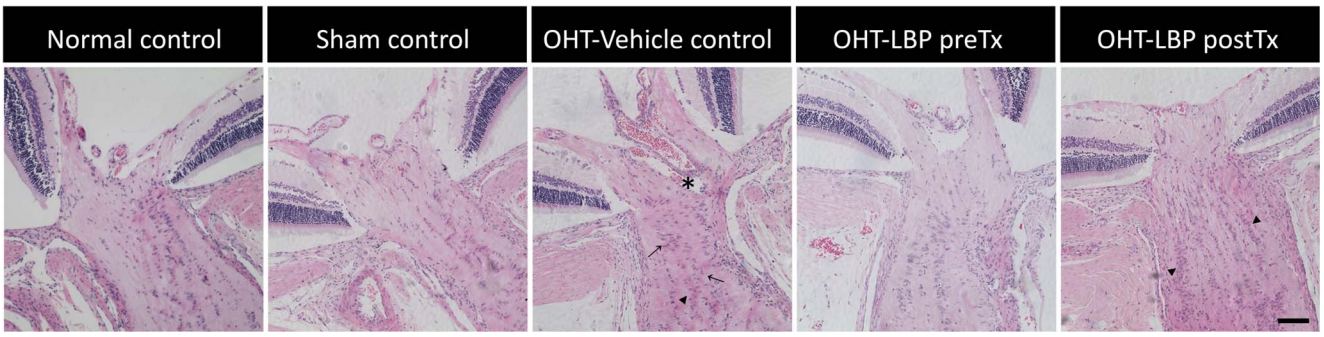

Figure 7. Representative ONH morphology from each experimental group at week 15. Upon OHT induction, the optic nerve of vehicle control showed loss of axon bundle structure (→) with enlarged and brightly stained cells (▲) and ONH cupping (*). LBP preTx preserved the axonal texture in the laminar region with no evidence of ONH cupping, comparable with the sham and the normal control. With posttreatment intervention, axon bundle arrangements looked preserved with the presence of enlarged and brightly stained cell. *Scale bars*: 100 µm.

Investigative Ophthalmology & Visual Science

with LBP (1 mg/kg) exerted long-term neuroprotective effects and preserved retinal structure (OCT and RGC counts) and function in a model of chronic OHT.

The circumlimbal suture placement around the limbus produced a moderate IOP elevation of approximately 50% in the first 3 to 4 weeks that was sustained throughout 15 weeks. It is worth noting that both pre- and posttreatment of LBP did not alter IOP as reported previously.[32] Cumulative IOP (over 15 weeks) was similar between the three OHT groups, and thus IOP-related stress was similar between these eyes. Also, IOP from the fellow control eyes of experimental groups were similar to naïve eyes of the sham control, demonstrating that the surgical procedure and suture placement for a day did not cause any lasting IOP changes.

On longitudinal evaluation, sham control (sutured removed after day 1) eyes showed no detectable changes in retinal and optic nerve structure or function and RGC density as compared with fellow naïve control eyes. In contrast, vehicle-treated OHT eyes developed a RNFL thinning (week 4, 15: –23 ± 15%, –17 ± 16 %), together with a reduced RGC density (–50 ± 15%, Fig. 6) and a disruption of axonal arrangement and posterior deformation of the optic nerve head (Fig. 7). Interestingly, both the IRL (IPL + INL: –9 ± 5%) and ORL (6 ± 4%) were thickened at week 15. IOP-induced thickening has been noted in experimental[48,49] and human glaucoma subjects,[48,50,51] with photoreceptors swelling[48] and glial proliferation[49,51,52] thought to be the primary drivers. Corresponding to RNFL thinning, functional measures of inner retina (week 15: pSTR: –39 ± 25%; b-wave: –23 ± 21%) and a-wave magnitudes (week 15: –38 ± 20%) were reduced. The decrease in photoreceptor response could have been resulted from a compromised choroidal blood flow to the outer retina, possibly arising directly from IOP elevation or indirectly from suture compressing the scleral and episleral plexus. Such deficits in choroidal blood flow along with the earlier reduction in a-wave followed by b-wave responses have been reported in mouse models of spontaneous glaucoma including DBA/2J[53] and DBA/2NNia.[54]

With pretreatment (week –1 to 15), LBP prevented much of the deficits in retinal structure and function induced by chronic IOP elevation. Most importantly, LBP delayed the onset and reduced RNFL thinning to –11 ± 9% at week 8 (–10 ± 12% at week 15) compared with –23 ± 15% thinning at week 4 in vehicle-control OHT eyes. LBP pretreatment also reduced the IRL and ORL thickening, which was seen in vehicle control. Pretreatment preserved RGC density and the optic nerve structure. The efficacy of pretreatment in preserving RGC density, was comparable to a previous report[32] in the laser photocoagulation chronic OHT model (in Sprague-Dawley rats) and 4 weeks of LBP dosing. LBP pretreatment preserved the RNFL thickness and also prevented functional deficits (pSTR, a- and b-waves) in OHT eyes, consistent with the protection of RGCs.

To evaluate posttreatment intervention, animals were fed with LBP from weeks 5 to 15. This time point was chosen after considering the following: (1) the pattern of compartmentalized neuronal degeneration reported in experimental glaucoma models,[55–57] and (2) the rate of structural and functional changes observed with the circumlimbal OHT approach in Sprague-Dawley rats.[44] As RNFL thinning was observable after 4 weeks of OHT induction, this was reasoned to be a good time point for LBP posttreatment intervention. In the LBP posttreatment group, OHT eyes showed RNFL loss at week 4 (–25 ± 12%), which was equivalent to the OHT-vehicle control (week 4: –23 ± 15%). With LBP intervention from week 5, there was no significant improvement in the rate of RNFL loss (week 15, –28 ± 9%). However, the raw data (see Supplementary Fig. S2) revealed a small increase in RNFL thickness in both OHT and fellow control eyes at week 8, which was sustained up through week 15. As LBP was administered orally, a corresponding increase in RNFLT in the fellow control could be attributed to the systemic effect of LBP or the contralateral eye effect. When calculating the rate of loss with respective to the fellow eyes, an equal increase in the thickness in these control eyes rendered no detectable change. However, the preservation of pSTR responses in OHT eyes until the end of the study corroborated with the increase in RNFL thickness. Also, LBP posttreatment improved the scotopic responses from week 8, which were otherwise decreased in vehicle control. LBP posttreatment also relatively prevented the RGC loss and ORL thickening. At weeks 12 and 15, the posttreatment functional benefits were similar to those of LBP pretreatment. One of the possible contributors for the improvement in RNFL thickness and retinal functions observed in the posttreatment could be attributed to the neuromodulatory effects of LBP on endothelin-1 (ET-1) and its receptors (ET-A, ET-B) located in the retinal neurons and its vasculature.[35] Increased levels of ET-1 in aqueous humor in patients with POAG[58] and ET-B receptor expression in the optic nerve of the postmortem glaucomatous eyes[59] have been reported. The potential role of ET-1 on the RGC loss has been further investigated by intraocular administration of ET-1[60–62] and experimental IOP elevation.[63,64] Under both conditions, there was a concomitant increase of ET-B receptor expression in the inner retinal layers, which was associated with a preferential apoptotic loss of RGCs. On the other hand, RGC loss was reduced when RGC-5 cells were pretreated with ET-B receptor antagonist[62] and in ET-B–deficient rats.[62,64] Furthermore, ET-1 was associated with a decreased ocular blood flow in animals[60] and human[65,66] and such reductions was inhibited by co-administrating ET-B receptor antagonist.[65] Treatment with Sulfisoxazole, a nonselective endothelin antagonist, improved ERG retinal functions in an acute ischemic insult model.[67] Because LBP pretreatment has shown to exert neuroprotective effects in a chronic OHT model by modulating ET-1, ET-A, and ET-B expressions in RGCs and the retinal vasculature,[35] we speculate that the protective effects on RFNL thickness and retinal function observed in the current study were mediated by similar mechanisms.

While no studies have reported posttreatment intervention with LBP, the results of the present study are comparable to a study using a similar OHT model (circumlimbal suture), in which IOP was normalized after 8 weeks of chronic IOP elevation by simply removing the suture.[68] In that study, RNFL loss was not progressive after suture removal (weeks 8 and 15: –10% and –11%) and GCL density was preserved with complete restoration of ganglion function loss at week 15 (7 weeks after normalizing IOP). While such reversal of neuronal dysfunction and structural preservation are attributable to IOP normalization, similar outcomes reported with LBP posttreatment in the presence of sustained IOP elevation suggest that IOP-independent factors are acting to preserve the retina.

The possible neuroprotective mechanisms of LBP in experimental glaucoma have been studied. First, LBP's dose-dependent neuroprotective effect on RGCs was associated with modulation of microglial activation.[33] Moderately activation of microglia using 1, 10, or 100 mg/kg LBP was protective; whereas excessive microglia activation with 1000 mg/kg was less neuroprotective. Pretreatment of LBP (1 mg/kg) may have direct neuroprotective effects on RGCs by upregulating crystalline proteins (found in the GCL and INL).[34] Indirect effects can arise from improved blood flow as evidenced by modulation of the expression of ET-1, and its receptors ET-A and ET-B in the GCL, INL, and retinal vasculature in OHT

eyes.[35] In other models of optic neuropathy LBP has also been shown to impact a range of pathways that can modify RGC survival, including activation of astrocytes (reduced glial fibrillary acidic protein), aquaporin-4 channels, poly(ADP-ribose) expression, the Nrf2/HO-1 antioxidant pathway, advanced glycation end products (AGE), and their receptors, amyloid-β proteins, c-jun N-terminal kinase pathway, and insulin-like growth factor-1.[36,37,39–41] The mechanisms involved in retinal protection with LBP posttreatment warrants further investigation.

Interestingly, the outcomes from the present chronic OHT study largely correspond with our earlier reports on pre- and posttreatment-LBP intervention using an acute OHT model.[46] Both studies showed that pretreatment LBP could prevent the initial stage of neuronal degeneration (dendritic and axonal loss) that arrested the subsequent events of somal loss, thus preserving the RNFLT and GCL density. Whereas, posttreatment LBP could not reverse the RNFL loss sustained prior to the intervention, but arrested later stages of neuronal degeneration and preserved the GCL density and maintained the retinal function. Thus, this study provides proof-of-concept evidence for translating LBP posttreatment as an adjunct glaucoma therapy, perhaps for those who show progressive loss of vision despite well-controlled IOP. To this end, further preclinical studies that simulate clinical study designs, which combine LBP treatment with IOP lowering therapy, are warranted.[42] Also, as glaucoma is prevalent among the geriatric population, the efficacy of LBP intervention should be considered in older rats.[43]

In summary, LBP pre- and posttreatment-exerted neuroprotective effects in a minimally invasive chronic OHT rat model that are independent of IOP lowering. Pretreatment with LBP offered superior neuroprotection as evidenced by longitudinal preservation of both inner and outer retinal structure and function. With posttreatment intervention, although LBP could not completely reverse the structural loss incurred prior to the treatment commencement, it arrested the subsequent neuronal degeneration and preserved the RGCs and retinal functions.

Acknowledgments

The authors thank Ricky Wing Kei Wu, School of Medical and Health Sciences, Tung Wah College, Hong Kong for availing their laboratory facilities to perform the histologic procedures. The authors also thank the University Research Facilities in Behavioural and Systems Neuroscience (UBSN) and in Life Sciences (ULS), The Hong Kong Polytechnic University for technical and facility supports.

Supported by grants from the General Research Fund (PolyU 151001/17M) from Research Grants Council, Hong Kong SAR, the Innovation and Technology Fund (P0012902) from the Innovation and Technology Commission (ITC), Hong Kong SAR, Central Research Grant (for Research Student), and Internal Research Grants (Z0GF) from The Hong Kong Polytechnic University, Hong Kong, SAR.

Disclosure: **Y. Lakshmanan**, None; **F.S.Y. Wong**, None; **B. Zuo**, None; **K.-F. So**, None; **B.V. Bui**, None; **H.H.-L. Chan**, None

References

1. Tham YC, Li X, Wong TY, Quigley HA, Aung T, Cheng CY. Global prevalence of glaucoma and projections of glaucoma burden through 2040: a systematic review and meta-analysis. *Ophthalmology*. 2014;121:2081–2090.
2. Adio AO, Onua AA. Economic burden of glaucoma in Rivers State, Nigeria. *Clin Ophthalmol*. 2012;6:2023–2031.
3. Lazcano-Gomez G, Ramos-Cadena ML, Torres-Tamayo M, Hernandez de Oteyza A, Turati-Acosta M, Jimenez-Román J. Cost of glaucoma treatment in a developing country over a 5-year period. *Medicine*. 2016;95:e5341–e5341.
4. Nayak B, Gupta S, Kumar G, Dada T, Gupta V, Sihota R. Socioeconomics of long-term glaucoma therapy in India. *Indian J Ophthalmol*. 2015;63:20–24.
5. Comparison of glaucomatous progression between untreated patients with normal-tension glaucoma and patients with therapeutically reduced intraocular pressures. *Am J Ophthalmol*. 1998;126:487–497.
6. Heijl A, Leske MC, Bengtsson B, Hyman L, Bengtsson B, Hussein M. Reduction of intraocular pressure and glaucoma progression: results from the Early Manifest Glaucoma Trial. *Arch Ophthalmol*. 2002;120:1268–1279.
7. Kass MA, Heuer DK, Higginbotham EJ, et al. The Ocular Hypertension Treatment Study: a randomized trial determines that topical ocular hypotensive medication delays or prevents the onset of primary open-angle glaucoma. *Arch Ophthalmol*. 2002;120:701–713.
8. Barkana Y, Belkin M. Neuroprotection in ophthalmology: a review. *Brain Res Bull* 2004;62:447–453.
9. Levin LA, Crowe ME, Quigley HA; Lasker/IRRF Initiative on Astrocytes and Glaucomatous Neurodegeneration Participants. Neuroprotection for glaucoma: requirements for clinical translation. *Exp Eye Res*. 2017;157:34–37.
10. Saccà SC, Pascotto A, Camicione P, Capris P, Izzotti A. Oxidative DNA damage in the human trabecular meshwork: clinical correlation in patients with primary open-angle glaucoma. *JAMA Ophthalmol*. 2005;123:458–463.
11. Feilchenfeld Z, Yücel YH, Gupta N. Oxidative injury to blood vessels and glia of the pre-laminar optic nerve head in human glaucoma. *Exp Eye Res*. 2008;87:409–414.
12. Gherghel D, Mroczkowska S, Qin L. Reduction in blood glutathione levels occurs similarly in patients with primary-open angle or normal tension glaucoma reduction in blood glutathione levels in glaucoma. *Invest Ophthalmol Vis Sci*. 2013;54:3333–3339.
13. Goyal A, Srivastava A, Sihota R, Kaur J. Evaluation of oxidative stress markers in aqueous humor of primary open angle glaucoma and primary angle closure glaucoma patients. *Curr Eye Res*. 2014;39:823–829.
14. Tezel G. Oxidative stress in glaucomatous neurodegeneration: mechanisms and consequences. *Prog Retin Eye Res*. 2006;25:490–513.
15. Harman D. Aging: a theory based on free radical and radiation chemistry. *J Gerontol*. 1956;11:298–300.
16. Harman D. Free radical theory of aging: an update: increasing the functional life span. *Ann N YAcad Sci*. 2006;1067:10–21.
17. Rhee DJ, Katz LJ, Spaeth GL, Myers JS. Complementary and alternative medicine for glaucoma. *Surv Ophthalmol*. 2001;46:43–55.
18. Rhee DJ, Spaeth GL, Myers JS, et al. Prevalence of the use of complementary and alternative medicine for glaucoma. *Ophthalmology*. 2002;109:438–443.
19. Wan MJ, Daniel S, Kassam F, et al. Survey of complementary and alternative medicine use in glaucoma patients. *J Glaucoma*. 2012;21:79–82.
20. Ho YS, So KF, Chang RC. Anti-aging herbal medicine–how and why can they be used in aging-associated neurodegenerative diseases? *Ageing Res Rev*. 2010;9:354–362.
21. Li X, Ma Y, Liu X. Effect of the Lycium barbarum polysaccharides on age-related oxidative stress in aged mice. *J Ethnopharmacol*. 2007;111:504–511.
22. Tang T, He B. Treatment of d-galactose induced mouse aging with Lycium barbarum polysaccharides and its mechanism study. *Afr J Tradit Complement Altern Med*. 2013;10:12–17.

23. Yu MS, Ho YS, So KF, Yuen WH, Chang RC. Cytoprotective effects of *Lycium barbarum* against reducing stress on endoplasmic reticulum. *Int J Mol Med*. 2006;17:1157–1161.
24. Cheng D, Kong H. The effect of *Lycium barbarum* polysaccharide on alcohol-induced oxidative stress in rats. *Molecules*. 2011;16:2542–2550.
25. Niu A-j, Wu J-m, Yu D-h, Wang R. Protective effect of *Lycium barbarum* polysaccharides on oxidative damage in skeletal muscle of exhaustive exercise rats. *Int J Biol Macromol*. 2008;42:447–449.
26. Wu H, Guo H, Zhao R. Effect of *Lycium barbarum* polysaccharide on the improvement of antioxidant ability and DNA damage in NIDDM rats. *Yakugaku Zasshi*. 2006; 126:365–371.
27. Cui B, Chen Y, Liu S, et al. Antitumour activity of *Lycium chinensis* polysaccharides in liver cancer rats. *Int J Biol Macromol*. 2012;51:314–318.
28. Gan L, Zhang SH, Yang XL, Xu HB. Immunomodulation and antitumor activity by a polysaccharide–protein complex from *Lycium barbarum*. *Int Immunopharmacol*. 2004;4:563–569.
29. Chen W, Cheng X, Chen J, et al. *Lycium barbarum* polysaccharides prevent memory and neurogenesis impairments in scopolamine-treated rats. *PLoS One*. 2014;9:e88076.
30. Hu X, Qu Y, Chu Q, Li W, He J. Investigation of the neuroprotective effects of *Lycium barbarum* water extract in apoptotic cells and Alzheimer's disease mice. *Mol Med Report*. 2018;17:3599–3606.
31. Yang D, Li S-Y, Yeung C-M, et al. *Lycium barbarum* extracts protect the brain from blood-brain barrier disruption and cerebral edema in experimental stroke. *PLoS One*. 2012;7: e33596.
32. Chan H-C, Chang RC-C, Ip AK-C, et al. Neuroprotective effects of *Lycium barbarum* Lynn on protecting retinal ganglion cells in an ocular hypertension model of glaucoma. *Exp Neurol*. 2007;203:269–273.
33. Chiu K, Chan H-C, Yeung S-C, et al. Modulation of microglia by wolfberry on the survival of retinal ganglion cells in a rat ocular hypertension model. *J Ocul Biol Dis Infor*. 2009;2:47–56.
34. Chiu K, Zhou Y, Yeung SC, et al. Up-regulation of crystallins is involved in the neuroprotective effect of wolfberry on survival of retinal ganglion cells in rat ocular hypertension model. *J Cell Biochem*. 2010;110:311–320.
35. Mi X-S, Chiu K, Van G, et al. Effect of *Lycium barbarum* polysaccharides on the expression of endothelin-1 and its receptors in an ocular hypertension model of rat glaucoma. *Neural Regen Res*. 2012;7:645–651.
36. He M, Pan H, Chang RC-C, So K-F, Brecha NC, Pu M. Activation of the Nrf2/HO-1 antioxidant pathway contributes to the protective effects of *Lycium barbarum* polysaccharides in the rodent retina after ischemia-reperfusion-induced damage. *PLoS One*. 2014;9:e84800.
37. Mi X-S, Feng Q, Lo ACY, et al. Protection of retinal ganglion cells and retinal vasculature by *Lycium barbarum* polysaccharides in a mouse model of acute ocular hypertension. *PLoS One*. 2012;7:e45469.
38. Chu PH, Li H-Y, Chin M-P, So K-f, Chan HH. Effect of *Lycium barbarum* (wolfberry) polysaccharides on preserving retinal function after partial optic nerve transection. *PLoS One*. 2013;8:e81339.
39. Li H, Liang Y, Chiu K, et al. *Lycium barbarum* (wolfberry) reduces secondary degeneration and oxidative stress, and inhibits JNK pathway in retina after partial optic nerve transection. *PLoS One*. 2013;8:e68881.
40. Li HY, Ruan YW, Kau PW, et al. Effect of *Lycium barbarum* (Wolfberry) on alleviating axonal degeneration after partial optic nerve transection. *Cell Transplant*. 2015;24:403–417.
41. Li S-Y, Yang D, Yeung C-M, et al. *Lycium barbarum* polysaccharides reduce neuronal damage, blood-retinal barrier disruption and oxidative stress in retinal ischemia/reperfusion injury. *PLoS One*. 2011;6:e16380.
42. Ergorul C, Levin LA. Solving the lost in translation problem: improving the effectiveness of translational research. *Curr Opin Pharmacol*. 2013;13:108–114.
43. Danesh-Meyer HV, Levin LA. Neuroprotection: extrapolating from neurologic diseases to the eye. *Am J Ophthalmol*. 2009; 148:186–191.
44. Lakshmanan Y, Wong F, Yu WY, et al. Characterization of circumlimbal suture induced chronic ocular hypertension in albino rats anaesthetised under Ketamine-Xylazine or Isoflurane. *Invest Ophthalmol Vis Sci*. 2018;59:3700–3700.
45. Yu M-S, Lai CS-W, Ho Y-S, et al. Characterization of the effects of anti-aging medicine Fructus lycii on β-amyloid peptide neurotoxicity. *Int J Mol Med*. 2007;20:261–268.
46. Lakshmanan Y, Wong FS, Yu WY, et al. *Lycium barbarum* polysaccharides rescue neurodegeneration in an acute ocular hypertension rat model under pre- and posttreatment conditions. *Invest Ophthalmol Vis Sci*. 2019;60:2023–2033.
47. Schlamp CL, Montgomery AD, Mac Nair CE, Schuart C, Willmer DJ, Nickells RW. Evaluation of the percentage of ganglion cells in the ganglion cell layer of the rodent retina. *Mol Vis*. 2013;19:1387–1396.
48. Nork TM, Ver Hoeve JN, Poulsen GL, et al. Swelling and loss of photoreceptors in chronic human and experimental glaucomas. *Arch Ophthalmol*. 2000;118:235–245.
49. Wilsey LJ, Reynaud J, Cull G, Burgoyne CF, Fortune B. Macular structure and function in nonhuman primate experimental glaucoma. *Invest Ophthalmol Vis Sci*. 2016;57:1892–1900.
50. Choi SS, Zawadzki RJ, Lim MC, et al. Evidence of outer retinal changes in glaucoma patients as revealed by ultrahigh-resolution in vivo retinal imaging. *Br J Ophthalmol*. 2011; 95:131–141.
51. Kim EK, Park H-YL, Park CK. Relationship between retinal inner nuclear layer thickness and severity of visual field loss in glaucoma. *Sci Rep*. 2017;7:5543.
52. Hood DC, Lin CE, Lazow MA, Locke KG, Zhang X, Birch DG. Thickness of receptor and post-receptor retinal layers in patients with retinitis pigmentosa measured with frequency-domain optical coherence tomography. *Invest Ophthalmol Vis Sci*. 2009;50:2328–2336.
53. Lavery WJ, Muir ER, Kiel JW, Duong TQ. Magnetic resonance imaging indicates decreased choroidal and retinal blood flow in the DBA/2J mouse model of glaucoma. *Invest Ophthalmol Vis Sci*. 2012;53:560–564.
54. Bayer AU, Neuhardt T, May AC, et al. Retinal morphology and ERG response in the DBA/2NNia mouse model of angle-closure glaucoma. *Invest Ophthalmol Vis Sci*. 2001;42:1258–1265.
55. Buckingham BP, Inman DM, Lambert W, et al. Progressive ganglion cell degeneration precedes neuronal loss in a mouse model of glaucoma. *J Neurosci*. 2008;28:2735–2744.
56. El-Danaf RN, Huberman AD. Characteristic patterns of dendritic remodeling in early-stage glaucoma: evidence from genetically identified retinal ganglion cell types. *J Neurosci*. 2015;35:2329–2343.
57. Weber AJ, Kaufman PL, Hubbard WC. Morphology of single ganglion cells in the glaucomatous primate retina. *Invest Ophthalmol Vis Sci*. 1998;39:2304–2320.
58. Tezel G, Kass MA, Kolker AE, Becker B, Wax MB. Plasma and aqueous humor endothelin levels in primary open-angle glaucoma. *J Glaucoma*. 1997;6:83–89.
59. Wang L, Fortune B, Cull G, Dong J, Cioffi GA. Endothelin B receptor in human glaucoma and experimentally induced optic nerve damage. *JAMA Ophthalmol*. 2006;124:717–724.

Investigative Ophthalmology & Visual Science

60. Chauhan BC, LeVatte TL, Jollimore CA, et al. Model of endothelin-1–induced chronic optic neuropathy in rat. *Invest Ophthalmol Vis Sci*. 2004;45:144–152.
61. Lau J, Dang M, Hockmann K, Ball AK. Effects of acute delivery of endothelin-1 on retinal ganglion cell loss in the rat. *Exp Eye Res*. 2006;82:132–145.
62. Krishnamoorthy RR, Rao VR, Dauphin R, Prasanna G, Johnson C, Yorio T. Role of the ETB receptor in retinal ganglion cell death in glaucoma. *Can J Physiol Pharmacol*. 2008;86:380–393.
63. Prasanna G, Hulet C, Desai D, et al. Effect of elevated intraocular pressure on endothelin-1 in a rat model of glaucoma. *Pharmacol Res*. 2005;51:41–50.
64. Minton AZ, Phatak NR, Stankowska DL, et al. Endothelin B receptors contribute to retinal ganglion cell loss in a rat model of glaucoma. *PLoS One*. 2012;7:e43199.
65. Polak K, Petternel V, Luksch A, et al. Effect of endothelin and BQ123 on ocular blood flow parameters in healthy subjects. *Invest Ophthalmol Vis Sci*. 2001;42:2949–2956.
66. Polak K, Luksch A, Frank B, Jandrasits K, Polska E, Schmetterer L. Regulation of human retinal blood flow by endothelin-1. *Exp Eye Res*. 2003;76:633–640.
67. Syed H, Safa R, Chidlow G, Osborne NN. Sulfisoxazole, an endothelin receptor antagonist, protects retinal neurones from insults of ischemia/reperfusion or lipopolysaccharide. *Neurochem Int*. 2006;48:708–717.
68. Liu HH, He Z, Nguyen CT, Vingrys AJ, Bui BV. Reversal of functional loss in a rat model of chronic intraocular pressure elevation. *Ophthalmic Physiol Opt*. 2017;37:71–81.

Investigative Ophthalmology & Visual Science